Mixed convection of power-law fluids along a vertical wedge with convective boundary condition in a porous medium [†]

Waqar A. Khan[1,*] and Rama Subba Reddy Gorla[2]

[1]*Department of Engineering Sciences, National University of Science and Technology, PNS Johar, Karachi 75350 Pakistan*
[2]*Department of Mechanical Engineering, Cleveland State University, Cleveland, Ohio, USA*

Abstract

The mixed convection of power-law fluids along a wedge in a porous medium is investigated numerically using an implicit finite difference method. Robin boundary condition is applied at the wedge surface. To explore the effects of mixed convection, both forced and free convection dominated regimes are considered separately. Non-similarity solutions are obtained for the variable heat transfer coefficient. Local dimensionless skin friction and Nusselt number are presented in tabular and graphical forms for the selected values of wedge and convective parameters. The wedge angle geometry parameter m, power index of pseudoplastic fluids n and mixed convection parameter ξ range from 0 to 1 in both regimes, whereas different values of convective parameter h_c are considered for investigating the behavior of skin friction and heat transfer rates.

Keywords: Mixed convection; Power-law fluids; Wedge; Porous medium; Finite difference method; Robin boundary condition

---

1. Introduction

In view of their wide applications in different industrial processes, and also by the interesting mathematical features presented their equations, boundary-layer flows of non-Newtonian fluids have motivated researchers in many branches of engineering in recent years. The most frequently used model in non-Newtonian fluid mechanics is the Ostwald-de Wael model (with a power-law rheology [1-4]), according to which the relationship between the shear stress and the strain rate is given as follows:

$$\tau_{xy} = \mu \left| \frac{\partial u}{\partial y} \right|^{n-1} \frac{\partial u}{\partial y}$$

For $n = 1$ the fluid is called Newtonian with dynamic coefficient of viscosity μ. For $n > 1$ the behavior of the fluid is dilatant or shear-thickening, and for $0 < n < 1$ the behavior is shear-thinning; in these cases the fluid is non-Newtonian and μ is the fluid consistency.

Mixed convection flows over wedge-shaped bodies are often encountered in many thermal engineering applications such as geothermal systems, crude oil extractions, ground water pollution, thermal insulation, heat exchanger and storage of nuclear waste etc.

Several studies exist for the mixed convection boundary layer flow about vertical, inclined and wedge surfaces immersed in a viscous fluid. The details of non-Newtonian fluids and mixed convection can be found in books [1-5] and in the literature [6-16]. In all these studies, the first and second kind of boundary conditions were applied at the surface. A non-similar solution of the mixed convection of power-law fluids along a wedge with the third kind of boundary condition could not be found in literature. The basic purpose of this study is to investigate the effects of the third kind of boundary condition (Robin boundary condition) on the local skin friction and dimensionless heat transfer rates along a wedge surface. We are concerned with the mixed convection of power-law fluids along a wedge with variable heat transfer coefficient in a porous medium. To cover the entire mixed convection regime, forced and free convection dominated regimes are studied separately. The transformed boundary layer equations are solved by means of an implicit finite difference method. Numerical results are obtained for skin friction coefficients $f''(\xi, 0)$ and local dimensionless heat transfer rates $\theta'(\xi, 0)$ for several values of power-law index.

2. Analysis

Consider steady mixed convection of power-law fluids along an impermeable vertical wedge (Fig. 1) heated by flow-

---

ing fluid at a temperature T_f with variable heat transfer coefficient [$h(x) = Ax^{-1/2}$, A is a specified constant] in a porous medium. If the temperature of the wedge surface and free stream differ, not only will energy be transferred to the flow but also density differences will exist. In a gravitational field, these density differences result in an additional force, namely, buoyancy force, besides viscous force due to viscous action. In many practical situations, the magnitudes of the buoyancy force and viscous force are of comparable order of magnitude and the convective heat transfer process is considered as mixed convection. Robin boundary condition is applied at the wedge surface. It is assumed that the Boussinesq approximation for the case of maximum density is valid. The pores of porous medium and the flow velocity are assumed to be small. The free stream velocity U_∞ is oriented in the upward direction and the ambient temperature is T_∞ as shown in Fig. 1, where x and y are the Cartesian coordinates along the wedge surface and normal to it, respectively. The velocity components are u along and v normal to the wedge surface. The acceleration due to gravity g acts vertically downwards opposite to the free stream velocity. The governing equations for this case can be written as

$$\frac{\partial u}{\partial x} + \frac{\partial v}{\partial y} = 0 \tag{1}$$

$$u^n = U_\infty^n + \frac{K}{v} g_x \beta(T - T_\infty) \tag{2}$$

$$u\frac{\partial T}{\partial x} + v\frac{\partial T}{\partial y} = \alpha \frac{\partial^2 T}{\partial y^2} \tag{3}$$

With boundary conditions

$$\left. \begin{array}{l} y = 0: \ v{=}0, \ -k\frac{\partial T}{\partial y} = h(x)(T_f - T) \\ y \to \infty: \ u \to U_\infty, \ T \to T_\infty \end{array} \right\} \tag{4}$$

where $g_x = g\cos\gamma$ in Eq. (2) is the x-component of the acceleration due to gravity. This problem is solved for two different regimes separately:
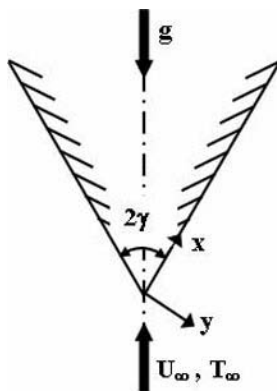

Fig. 1. Flow model and coordinate system.

2.1 Forced convection dominated regime

Define a stream function $\psi(x, y)$ such that

$$u = \frac{\partial \psi}{\partial y} \quad \text{and} \quad v = -\frac{\partial \psi}{\partial x} \tag{5}$$

and the following transformations

$$\left. \begin{array}{ll} \eta = \dfrac{y}{x} Pe_x^{1/2} & \psi = \alpha Pe_x^{1/2} f(\xi_f, \eta) \\[2mm] \xi_f = \left(\dfrac{Ra_x}{Pe_x}\right)^n & \theta = \dfrac{T - T_\infty}{T_f - T_\infty} \\[2mm] Pe_x = \dfrac{U_\infty x}{\alpha} & Ra_x = \dfrac{x}{\alpha}\left[\dfrac{Kg_x \beta(T_f - T_\infty)}{v}\right]^{1/n} \\[2mm] U_\infty = Cx^m & m = \dfrac{\gamma}{\pi - \gamma} \end{array} \right\} \tag{6}$$

Using these transformations, the above governing equations become

$$(f')^n = 1 + \xi_f \theta \tag{7}$$

$$\theta'' + \left(\frac{m+1}{2}\right) f\theta' = -m\xi_f \left[f'\frac{\partial\theta}{\partial\xi_f} - \theta'\frac{\partial f}{\partial\xi_f} \right] \tag{8}$$

with transformed boundary conditions

$$\left. \begin{array}{ll} f(\xi_f, 0) = 0 & \theta'(\xi_f, 0) = -h_c\left[1 - \theta(\xi_f, 0)\right] \\ f'(\xi_f, \infty) = 1 & \theta(\xi_f, \infty) = 0 \end{array} \right\} \tag{9}$$

where $h_c = \dfrac{A}{k}\sqrt{\alpha/U_\infty}$ is the convective parameter, and f' and θ' are the partial derivatives w.r.t. η. The local skin friction and dimensionless heat transfer coefficients are given by

$$C_f = f''(\xi_f, 0) = \frac{\xi_f}{n} \frac{f'(\xi_f, 0)\theta'(\xi_f, 0)}{1 + \xi_f \theta(\xi_f, 0)} \tag{10}$$

$$\frac{Nu(\xi_f, 0)}{Pe_x^{1/2}} = -\theta'(\xi_f, 0) \tag{11}$$

The dimensionless parameter ξ_f measures the effect of buoyancy on forced convection. For pure forced convection, $\xi_f = 0$, which reduces Eqs. (7) and (8) to a single governing equation for all values of n.

$$\theta'' + \left(\frac{m+1}{2}\right)\eta\theta' = 0 \tag{12}$$

With boundary conditions

Table 1. Analytical solutions for selected values of wedge parameter m.

m	$\theta(\eta)$
0	$\dfrac{h_c\sqrt{\pi}\left[1-erf(\eta/2)\right]}{1+h_c\sqrt{\pi}}$
1/3	$\dfrac{3h_c\sqrt{\pi}\left[1-erf\left(\eta/\sqrt{3}\right)\right]}{2\sqrt{3}+3h_c\sqrt{\pi}}$
1/2	$\dfrac{2h_c\sqrt{\pi}\left[1-2erf\left(\sqrt{6}\eta/4\right)\right]}{\sqrt{6}+2h_c\sqrt{\pi}}$
1	$\dfrac{h_c\sqrt{\pi}\left[1-erf\left(\eta/\sqrt{2}\right)\right]}{\sqrt{2}+h_c\sqrt{\pi}}$

Table 2. Local dimensionless heat transfer values for pure forced convection ($\xi_f = 0$) along a wedge.

h_c	$-\theta'(\xi_f,0)$			
	$m=0$	$m=1/3$	$m=1/2$	$m=1$
0.05	0.0459	0.0464	0.0466	0.0471
0.1	0.0849	0.0867	0.0874	0.0889
0.2	0.1477	0.1530	0.1551	0.1599
0.4	0.2341	0.2478	0.2533	0.2664
0.6	0.2908	0.3123	0.3211	0.3425
0.8	0.3309	0.3591	0.3708	0.3995
1	0.3607	0.3945	0.4086	0.4438
5	0.5070	0.5764	0.6071	0.6881
10	0.5341	0.6116	0.6463	0.7389
20	0.5487	0.6309	0.6679	0.7673
30	0.5538	0.6376	0.6754	0.7772
40	0.5563	0.6410	0.6793	0.7823
50	0.5579	0.6431	0.6816	0.7854

$$\theta'(0) = -h_c\left[1-\theta(0)\right], \qquad \theta(\infty)=0 \tag{13}$$

It is interesting to note that Eq. (12) is independent of index n and has analytical solutions for all fluids (as shown in Table 1). The numerical results of local dimensionless heat transfer rates for the selected values of the wedge and convective parameters are presented in Table 2.

For the mixed convection regime, Eqs. (7) and (8) with boundary conditions (9) are solved by using an implicit finite difference method as described by Gorla and Kumari [9]. Numerical results of local skin friction and dimensionless heat transfer rates are presented in Table 3 for $h_c = 10$ and the selected values of wedge parameter and power-law index n for pseudoplastic fluids. It is observed that both the skin friction and heat transfer values increase with the increase in both wedge and mixed convection parameters but decrease with the increase in power-law index for pseudoplastic fluids. As the convective parameter h_c increases, the heat transfer rates approach to the constant temperature case. This statement is also supported by the first boundary condition of (13), which gives $\theta(0)=1$ as $h_c \to \infty$.

2.2 Free convection dominated regime

Using the following transformations for free convection dominated regime,

$$\left.\begin{array}{ll} \eta = \dfrac{y}{x}Ra_x^{1/2} & \psi = \alpha Ra_x^{1/2}f(\xi_n,\eta) \\[2mm] \xi_n = \left(\dfrac{Pe_x}{Ra_x}\right)^n & \theta(\xi_n,\eta) = \dfrac{T-T_\infty}{T_f - T_\infty} \end{array}\right\} \tag{14}$$

Eqs. (1-3) reduce to

$$(f')^n = \xi_n + \theta \tag{15}$$

$$\theta'' + \left(\frac{1}{2}\right)f\theta' = m\xi_n\left[f'\frac{\partial\theta}{\partial\xi_n} - \theta'\frac{\partial f}{\partial\xi_n}\right] \tag{16}$$

with transformed boundary conditions

$$\left.\begin{array}{ll} f(\xi_n,0)=0 & \theta'(\xi_n,0) = -h_c\left[1-\theta(\xi_n,0)\right] \\[2mm] f'(\xi_n,\infty)=\xi & \theta(\xi_n,\infty)=0 \end{array}\right\} \tag{17}$$

In this regime, local dimensionless skin friction and heat transfer coefficients are given by

$$C_f = f''(\xi_n,0) = \frac{1}{n}\frac{f'(\xi_n,0)\theta'(\xi_n,0)}{\xi_n + \theta(\xi_n,0)} \tag{18}$$

$$\frac{Nu(\xi_n,0)}{Ra_x^{1/2}} = -\theta'(\xi_n,0) \tag{19}$$

The controlling parameter ξ_n determines the forced flow effect on free convection. For pure free convection, $\xi_n = 0$ whereas in the limiting case $\xi_n \to \infty$ it corresponds to pure forced convection. For pure free convection, Eqs. (15) and (16) reduce to

$$(f')^n - \theta = 0 \tag{20}$$

$$\theta'' + \left(\frac{1}{2}\right)f\theta' = 0 \tag{21}$$

With boundary conditions

$$\left.\begin{array}{ll} f(0)=0 & \theta'(0) = -h_c\left[1-\theta(0)\right] \\[2mm] f'(\infty)=0 & \theta(\infty)=0 \end{array}\right\} \tag{22}$$

It is interesting to note that Eq. (21) is independent of the wedge parameter m. The results for the local dimensionless skin friction and heat transfer coefficients in case of pure free convection are presented in Table 4.

For the case of $h_c \to \infty$ and $n=1$, Gorla and Kumari [9] reported $-\theta'(0) = 0.4436$, whereas the present value of $-\theta'(0)$ is 0.4387 for $h_c = 50$. This would suggest that the present numerical values are highly accurate.

Table 3. Effect of buoyancy on local skin friction and heat transfer coefficients of pseudoplastic fluids along wedge for $h_c = 10$ and different wedge parameters.

n	ξ_f	$m = 1/3$		$m = 1/2$		$m = 1$	
		$-\theta'(\xi_f, 0)$	$-f''(\xi_f, 0)$	$-\theta'(\xi_f, 0)$	$-f''(\xi_f, 0)$	$-\theta'(\xi_f, 0)$	$-f''(\xi_f, 0)$
1.0	0	0.6116	0.0000	0.6463	0.0000	0.7389	0.0000
	0.1	0.6285	0.0629	0.6640	0.0664	0.7587	0.0759
	0.2	0.6447	0.1289	0.6810	0.1362	0.7778	0.1556
	0.3	0.6603	0.1981	0.6974	0.2092	0.7961	0.2388
	0.4	0.6755	0.2702	0.7133	0.2853	0.8139	0.3256
	0.5	0.6902	0.3451	0.7287	0.3643	0.8311	0.4155
	0.6	0.7044	0.4227	0.7436	0.4462	0.8477	0.5087
	0.7	0.7183	0.5028	0.7581	0.5307	0.8646	0.6052
	0.8	0.7318	0.5854	0.7722	0.6178	0.8797	0.7038
	0.9	0.7449	0.6704	0.7860	0.7074	0.8950	0.8055
	1	0.7577	0.7577	0.7994	0.7994	0.9100	0.9100
0.5	0	0.6116	0.0000	0.6463	0.0000	0.7389	0.0000
	0.1	0.6458	0.1412	0.6821	0.1491	0.7790	0.1702
	0.2	0.6796	0.3225	0.7176	0.3403	0.8186	0.3876
	0.3	0.7131	0.5470	0.7526	0.5768	0.8577	0.6557
	0.4	0.7461	0.8179	0.7872	0.8619	0.8962	0.9780
	0.5	0.7789	1.1380	0.8214	1.1984	0.9342	1.3577
	0.6	0.8112	1.5101	0.8552	1.5893	0.9716	1.7976
	0.7	0.8431	1.9370	0.8885	2.0374	1.0088	2.3012
	0.8	0.8747	2.4212	0.9215	2.5452	1.0450	2.8697
	0.9	0.9059	2.9652	0.9540	3.1153	1.0808	3.5072
	1	0.9367	3.5714	0.9861	3.7500	1.1162	4.2156
0.2	0	0.6116	0.0000	0.6463	0.0000	0.7389	0.0000
	0.1	0.7008	0.5001	0.7398	0.5271	0.8433	0.5986
	0.2	0.7962	1.5650	0.8394	1.6452	0.9539	1.8552
	0.3	0.8968	3.5338	0.9443	3.7043	1.0695	4.1462
	0.4	1.0018	6.8532	1.0535	7.1628	1.1891	7.9562
	0.5	1.1104	12.0851	1.1660	12.5932	1.3114	13.8800
	0.6	1.2215	19.9086	1.2809	20.6826	1.4355	22.6193
	0.7	1.3345	31.1166	1.3974	32.2284	1.5605	34.9750
	0.8	1.4485	46.6097	1.5148	48.1302	1.6856	51.8363
	0.9	1.5631	67.3862	1.6323	69.3791	1.8102	74.1685
	1	1.6775	94.5299	1.7494	97.0450	1.9337	102.9988

3. Numerical Scheme

The numerical scheme to solve Eqs. (7) and (8) adopted here is based on a combination of the following concepts:

The boundary conditions for $\eta = \infty$ are replaced by

$$f'(\xi, \eta_{max}) = 1, \quad \text{and} \quad \theta(\xi, \eta_{max}) = 0 \tag{23}$$

Where η_{max} is a sufficiently large value of η at which the boundary conditions (23) are satisfied. In this problem, $\eta_{max} = 20$.

The two-dimensional domain of interest (ξ, η) is discretized with an equispaced mesh in the ξ – direction and an-other equispaced mesh in the η – direction.

The partial derivatives with respect to η and ξ are evaluated by the central difference approximations.

Two iteration loops based on the successive substitution are used because of the non-linearity of the equations.

In each inner iteration loop, the value of ξ is fixed while each of the Eqs. (7) and (8) is solved as a linear second order boundary value problem of ODE in the η – domain. The inner iteration is continued until the non-linear solution converges for the fixed value of ξ.

In the outer iteration loop, the value of ξ is advanced from 0 to 100. The derivatives with respect to ξ are updated after every outer iteration step.

Table 4. Local skin friction and dimensionless heat transfer rates for pure free convection $(\xi_n = 0)$ of pseudoplastic fluids along a wedge.

h_c	$n = 1$		$n = 0.5$	
	$-\theta'(0)$	$-f''(0)$	$-\theta'(0)$	$-f''(0)$
0.05	0.0404	0.0404	0.0375	0.0188
0.1	0.0713	0.0713	0.0635	0.0464
0.5	0.2039	0.2039	0.1712	0.2251
1	0.2752	0.2752	0.2298	0.3540
5	0.3934	0.3934	0.3325	0.6207
10	0.4171	0.4171	0.3543	0.6836
20	0.4303	0.4303	0.3667	0.7200
30	0.4350	0.4350	0.3711	0.7329

In the inner iteration step, the finite difference approximation for Eqs. (7) and (8) is solved as a boundary value problem. We consider Eq. (7) first. By defining $f = \phi$, Eq. (7) may be written in the form

$$a_1 \phi'' + b_1 \phi' + c_1 \phi = S_1 \qquad (24)$$

where $a_1 = 0, b_1 = 1, c_1 = 0$, and $S_1 = 1 + \xi_f \theta$.

The coefficients a_1, b_1, c_1 and the source term S_1 in Eq. (24), in the inner iteration step are evaluated by using the solution from the previous iteration step. Eq. (24) is then transformed to a finite difference equation by applying the central difference approximations to the first and second derivatives. The finite difference equations form a diagonal system and can be solved by the tridiagonal solution scheme.

Eq. (8) is also written as a second-order boundary value problem similar to Eq. (24):

$$a_2 \phi'' + b_2 \phi' + c_2 \phi = S_2 \qquad (25)$$

Where $a_2 = 1, b_2 = \dfrac{m+1}{2}\phi, c_2 = 0$, and

$$S_2 = -m\xi_f \left[\phi' \frac{\partial \theta}{\partial \xi_f} - \theta' \frac{\partial \phi}{\partial \xi_f} \right].$$

The numerical results are affected by the number of mesh points in both directions. To obtain accurate results, a mesh sensitivity study was performed. After some trials, in the η – direction 190 mesh points were selected, whereas in the ξ – direction, 4001 mesh points were used.

4. Results and discussion

Local skin friction coefficients at the wedge surface are shown in Fig. 2 for both forced and free convection dominated regimes for the selected values of wedge m and convective h_c parameters. It can be seen in Fig. 2(a) and (b) that as the value of n decreases, skin friction increases in both regimes with the mixed convection parameter ξ. This is due to the fact
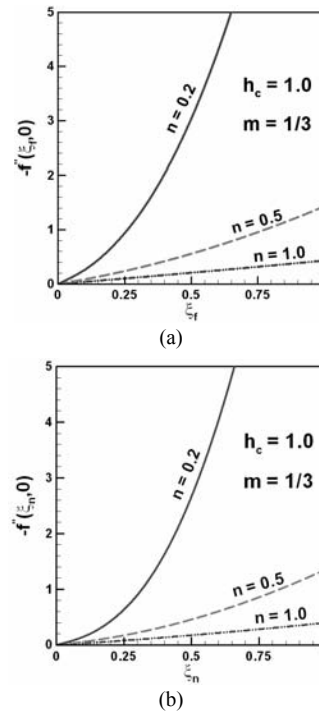

(a)

(b)

Fig. 2. Local skin friction for (a) forced convection dominated region and (b) free convection dominated region.

that skin friction depends strongly on the parameter n. Power-law fluids display higher wall friction. It is also observed that the skin friction increases with the wedge parameter m and the mixed convection parameter ξ. From the numerical results, we note that the friction factor increases as the wedge angle increases. As the buoyancy increases, the friction factor increases. Local dimensionless heat transfer rates at the wedge surface are shown in Fig. 3 in both regimes for the selected values of h_c, m and the power-law index n. It can be seen that the heat transfer rates increase with the increase in all the three parameters. As the effects of buoyancy on forced convection ξ_f (Fig. 3(a)) or the forced flow on free convection ξ_n (Fig. 3(b)) increases, the local dimensionless heat transfer rates increase sharply for all pseudoplastic fluids. In the free convection dominated regime, the local heat transfer values are smaller for the smaller values of power-law index when the effect of forced flow on free convection is low. But as this effect increases, the heat transfer rate values become larger for smaller power-law index. As the buoyancy increases, the heat transfer rates get augmented. As the wedge angle increases, the heat transfer rates increase. As the surface convective heat transfer coefficient increases, heat transfer rates increase, which is expected because of the increased molecular activity near the surface as the heat transfer coefficient increases.

5. Conclusions

Mixed convection of power-law fluids along a vertical wedge in a porous medium is investigated numerically using an implicit finite difference method. The boundary layer equa-
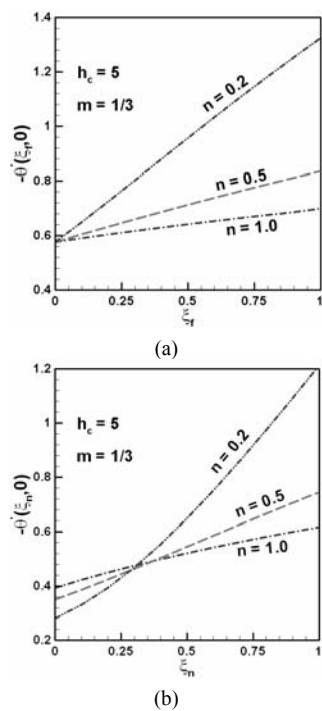
Fig. 3. Local dimensionless heat transfer for (a) forced convection dominated region and (b) free convection dominated.

tions are solved in both forced and free convection dominated regimes and non-similar solutions are obtained for selected values of n, m, and h_c. Due to the unavailability of previous results in the literature, the present values of skin friction and heat transfer rates could not be compared. However, these values approach the constant temperature boundary condition as the convective parameter approaches to infinity. The results of local skin friction and dimensionless heat transfer rates are tabulated (Table 3) in the forced convection dominated regime and graphically presented (Figs. 3 and 4) as well. It is shown that both skin friction and dimensionless heat transfer rates depend strongly on the power-law index and convective parameter.

Nomenclature————————————————————

A	:	Constant
C_f	:	Skin friction
f	:	Dimensionless stream function
g	:	Acceleration due to gravity [m/s²]
h_c	:	Convective parameter
h	:	Heat transfer coefficient [W/m²·K]
K	:	Permeability for porous medium
m	:	Wedge flow parameter
n	:	Power-law index (< 1 for pseudoplastic fluids)
Nu	:	Nusselt number
Pex	:	Local Peclet number
Ra_x	:	Local Rayleigh number
T	:	Temperature [ºC]
U_∞	:	Free stream velocity [m/s]

u, v	:	Velocity components in x- and y- direction
x, y	:	Coordinates along and normal to wedge surface

Subscripts

f	:	Forced convection dominated regime
∞	:	Free stream conditions
n	:	Free convection dominated regime
w	:	Wall

Greek Symbols

α	:	Thermal diffusivity of porous medium [m²/s]
β	:	Volumetric coefficient of expansion [1/K]
η	:	Similarity variable
γ	:	Semi wedge angle
μ	:	Absolute viscosity [kg/ms]
v	:	Kinematic viscosity [m²/s]
ρ	:	Fluid density [kg/m³]
ψ	:	Stream function
θ	:	Dimensionless temperature
ξ	:	Mixed convection parameter

References

[1] R. P. Chhabra and J. F. Richardson, Non-Newtonian Flow and Applied Rheology: *Engineering applications*, Pergamon, Oxford, 2008.

[2] R. P. Chhabra and J. F. Richardson, Non-Newtonian Flow in the Process Industries: *Fundamentals and Engineering Applications*, Butterworth-Heinemann, Oxford, 1999.

[3] D. A. Nield and A. Bejan, Convection in Porous Media, Second Ed., Springer, New York, 1999.

[4] D. B. Ingham and I. Pop, Transport Phenomena in Porous Media, Vol. 2, Pergamon, Oxford, 2002.

[5] I. Pop and D. B. Ingham, Convective Heat Transfer: Computational and Mathematical Modelling of Viscous Fluids and Porous Media, Pergamon, Oxford, 2001.

[6] I. A. Hassanien, Variable permeability effects on mixed convection along a vertical wedge embedded in a porous medium with variable surface heat flux, *Appl Math Comp*, 138 (2003) 41-59.

[7] I. A. Hassanien, A. H. Essawy and N. M. Moursy, Variable viscosity and thermal conductivity effects on combined heat and mass transfer in mixed convection over a UHF/UMF wedge in porous media: The entire regime, *Appl Math Comp*, 145 (2003) 667-682.

[8] F. S. Ibrahim and I. A. Hassanien, Influence of variable permeability on combined convection along a non-isothermal wedge in a saturated porous medium, Transport Porous Med, 39 (2000) 5771, 2000.

[9] R. S. R. Gorla and M. Kumari, Non-similar solutions for mixed convection in non-Newtonian fluids along a wedge with variable surface temperature in a porous medium, Int J Numer Method H, 9 (5) (1999) 601-611.

[10] J. C. Hsieh, T. S. Chen and B. F. Armaly, Non-similarity

solutions for mixed convection from vertical surfaces in porous media: Variable surface temperature or heat flux, Int J Heat Mass Tran, 36 (6) (1993) 1485-1493.

[11] P. Cheng, Combined free and forced convection flow about inclined surfaces in porous Media,Int. J. Heat Mass Tran, 20 (8) (1977) 807-814.

[12] J. V. C. Vargas, T. A. Laursen and A. Bejan, Non-similar solutions for mixed convection on a wedge embeded in a porous medium, Int. J. Heat Fluid Fl, 16 (1995) 211-216.

[13] S. Bhattacharyya, A. Pal and I. Pop, Unsteady mixed convection on a wedge in a porous medium, Int Commun Heat Mass, 25 (5) (1998) 743-752.

[14] M. A. Hossain, S. Bhowmick and R. S. R. Gorla, Unsteady mixed-convection boundary layer flow along a symmetric wedge with variable surface temperature, Int. J. Eng. Sci. 44 (2006) 607-620.

[15] P. Ranganathan and R. Viskanta, Mixed convection boundary layer flow along a vertical surface in a porous medium, Num. Heat Transfer, 7 (1984) 305-317.

[16] C. H. Chen, T. S. Chen and C. K. Chen, Non-Darcy mixed convection along non-isothermal vertical surfaces in porous media, Int. J. Heat Mass Tran, 39 (1996) 1157-1164.

Waqar Ahmad Khan is a Professor of Mechanical Engineering at the National University of Sciences and Technology, Pakistan. Dr. Khan received a B.E. in Mechanical Engineering from NED University of Engineering and Technology, Pakistan in 1982, M. A. in Applied Mathematics from Karachi university in 1988, M.E. in Mechanical Engineering from the Stevens Institute of Technology, New Jersey, USA. in 1996 and Ph.D. in Mechanical Engineering from the University of Waterloo in 2004. Dr. Khan has developed several unique analytical models for the fluid flow and heat transfer across single cylinders (circular/elliptical), tube banks and pin-fin heat sinks to Newtonian and Non-Newtonian fluids. Dr. Khan has more than 45 publications in refereed journals and international conferences.

Rama Gorla is Fenn Distinguished Research Professor in the Department of Mechanical Engineering at Cleveland State University. He received the Ph.D. in Mechanical Engineering from the University of Toledo in 1972. His primary research areas are combustion, heat transfer and fluid dynamics. He has been recently involved in the testing and development of a three-dimensional Navier Stokes Computational Code for Wright Patterson Air Force Base. He worked as a turbomachinery design engineer at Teledyne Continental Motors Turbine Engines (TCM-TE) in Toledo, Ohio and as a design engineer of the aerothermodynamics of rotating machinery at Chrysler Corporation in Highland Park, Michigan. Dr. Gorla has published over 400 technical papers in refereed journals and contributed several book chapters in Encyclopedia of Fluid Mechanics.